Unclassified

Technical Report No. 248

Application of the Resonant Cavity Method to the Measurement of Electron Densities and Collision Frequencies in the Wakes of Hypervelocity Pellets

M. Labitt
M. A. Herlin

17 October 1961

Lincoln Laboratory
MASSACHUSETTS INSTITUTE OF TECHNOLOGY

Unclassified

The work reported in this document was performed at Lincoln Laboratory, a center for research operated by Massachusetts Institute of Technology; this work was supported by the U.S. Advanced Research Projects Agency under Air Force Contract AF 19(604)-7400 (ARPA Order 13-61).

MASSACHUSETTS INSTITUTE OF TECHNOLOGY
LINCOLN LABORATORY

APPLICATION OF THE RESONANT CAVITY METHOD TO THE MEASUREMENT OF ELECTRON DENSITIES AND COLLISION FREQUENCIES IN THE WAKES OF HYPERVELOCITY PELLETS

M. LABITT

M. A. HERLIN

Group 35

TECHNICAL REPORT NO. 248

17 OCTOBER 1961

ABSTRACT

The use of the resonant cavity method for measuring electron densities and collision frequencies in the ionized wakes of hypervelocity pellets is described. The equivalent circuit obtained from a normal mode analysis of the cavity fields and their interaction with the wake plasma is used to determine the plasma parameters in terms of measurable properties of the cavity. The range of validity of the method is discussed, along with a sensitivity and accuracy analysis.

LEXINGTON MASSACHUSETTS

DEFINITIONS OF SYMBOLS

Symbol	Defined in Connection with Equation Number	
B_c	(1)	Cavity susceptance referred to cavity end plates
B_e	(1), (10), (12), (13b)	Plasma susceptance referred to cavity end plates
c		Velocity of light in free space, 2.9979×10^8 meters/second
C_c	(1), (2), (5)	Effective cavity capacitance referred to end plates
C_s	(30)	Series end-effect capacitance referred to cavity end plates
e		Electron charge, 1.602×10^{-19} coulomb
E	(1)	Electric field in cavity
E_a	(1)	Unperturbed electric field in cavity
E_i	(35)	Internal field of spheroid
E_o	(1)	Electric field in center of cavity
g	(43)	Fractional energy loss of electron in collision
G_c	(1)	Intrinsic ohmic loss conductance of cavity referred to end plates
G_d	(1)	Detector conductance referred to cavity end plates
G_e	(1), (10), (12), (13a)	Plasma conductance referred to cavity end plates
$G_g = 1/R_g$	(1)	Generator conductance referred to cavity end plates
$G_L = G_c + G_d + G_g$	(14)	
$j = \sqrt{-1}$		Imaginary operator
J	(1)	Plasma conduction current density
J_o, J_1	(3)	Zero- and first-order Bessel functions
$J_1^2(\alpha) = 0.2695$	(3)	
k		Boltzmann's constant, 1.38×10^{-23} joule/degree
ℓ	(33)	Depolarizing factor
L_c	(2)	Effective cavity inductance referred to end plates

Symbol	Defined in Connection with Equation Number	
m		Electron mass, 9.108×10^{-31} kilogram
M	(43)	Molecule mass
n	(11)	Electron volume density
N	(12)	Electron line density
N_{max}	(51)	Maximum detectable electron line density
N_{min}	(48)	Minimum detectable electron line density
P_i	(44)	Incident power from signal generator
$Q_c = \omega_o C_c / G_c$	(7)	Unloaded Q of cavity
$Q_d = \omega_o C_c / G_d$	(9)	External Q of detector output
$Q_g = \omega_o C_c / G_g$	(8)	External Q of generator "output"
$Q_L = \omega_o C_c / G_L$	(14)	Total loaded Q of cavity
r	(3)	Radial coordinate in cavity
R_g	(1)	Generator impedance (resistance) referred to cavity end plates
$S = \lvert V/V_o \rvert$	(16a, b)	
T_d	(45)	Detector noise temperature
Δu	(43)	Increase of electron energy due to balance between field heating and collision cooling
Δu_E	(43)	Change of electron energy per collision due to electric field
Δu_c	(43)	Change of electron energy per collision due to molecule recoil and excitation
U	(3)	Energy stored in cavity
v_c	(1)	Cavity volume
V	(1)	Cavity output voltage referred to end plates
V_g	(1)	Generator emf referred to cavity end plates
V_n	(45)	Receiver noise voltage referred to cavity end plates
V_o	(15)	V in absence of plasma, equal to Thevenin equivalent generator emf
$Y_c = G_c + jB_c$	(1)	Intrinsic admittance of cavity referred to end plates

Symbol	Defined in Connection with Equation Number	
Y_{chg}	(1)	Characteristic admittance of generator output referred to cavity end plates
$Y_e = G_e + jB_e$	(1), (10), (12)	Plasma admittance referred to cavity end plates
Y'_e	(36)	Admittance of plasma conductance in series with end-effect capacitance
Y_g	(1)	Cavity input admittance referred to end plates
Z_{ch}	(39)	Characteristic impedance of slow-wave line
$\alpha = 2.405$	(3)	Argument at first zero of Bessel function of zero order
δ	(1)	Length of cavity
δ_s	(30)	Length of coaxial capacitance
ϵ	(37)	Naperian logarithm base, 2.718...
ϵ_o		Electric permittivity of free space, 8.85×10^{-12} farad/meter
$\mathcal{E}$	(33)	Spheroid eccentricity
Θ	(17)	Phase angle of V relative to that of V_o
κ	(23)	Effective dielectric coefficient of plasma
λ	(29b)	Free-space wavelength
μ_o		Magnetic permeability of free space, $4\pi \times 10^{-7}$ henry/meter
ν_m	(11)	Electron-molecule collision frequency for momentum transfer
ρ	(3)	Cavity radius
ρ_e	(12)	Plasma radius
ρ_p	(30)	Portal radius
σ	(11)	Plasma conductivity
σ_i	(11)	Imaginary part of σ
σ_r	(11)	Real part of σ
τ	(45)	Detector response time
ω	(1)	Radian frequency of generator
ω_o	(1)	Cavity resonant radian frequency
ω_p	(26)	Plasma frequency

APPLICATION OF THE RESONANT CAVITY METHOD TO THE MEASUREMENT OF ELECTRON DENSITIES AND COLLISION FREQUENCIES IN THE WAKES OF HYPERVELOCITY PELLETS

I. INTRODUCTION AND REQUIREMENTS

The properties of ionized wakes caused by the passage of hypervelocity bodies may be studied in the laboratory by means of the two-stage light-gas gun. A central problem in this study is the measurement of electron density. This problem has been studied in connection with plasmas generated by other means, such as electrical discharges in gases. One of the most satisfactory techniques has proved to be the measurement of the complex input or transfer admittance of a resonant cavity that contains the ionized gas in a high-electric-field region of the cavity.[1,2] This report describes the capabilities, precautions and limitations of the cavity technique applied to the investigation of hypervelocity wakes.

The measurement system design must take account of four features of hypervelocity pellet experiments which are frequently not met in other applications of the cavity method:

(a) Entrance and exit ports must be provided to permit free passage of the pellet and to measure a segment of a long wake without loss of control of the electromagnetic environment.

(b) The presence of the cavity structure must not be permitted to modify sensibly the flow pattern of the wake gases or otherwise modify the plasma under measurement.

(c) The cavity construction must be rugged enough to withstand the mechanical deformations produced by shock waves and other stresses caused by the hypervelocity flight and firing of the gun.

(d) Data presentation and recording must be accomplished on a single-sweep basis.

II. CAVITY DESIGN

The cavity employed in recent experiments is shown schematically in Fig. 1, and photographically in Fig. 2. It resonates in the TM_{010} mode. Entry and exit ports are provided in the circular disk ends, with lengths of circular tubing beyond propagation cutoff to prevent coupling of RF energy from the cavity to the region outside. This method is suitable in the absence of the wake plasma, but must be reconsidered when the pellet and wake pass through and create a possible propagating mode of the coaxial type. This question is discussed later. The cavity is cast with heavy walls, especially the end plates, and with ribbing as shown. The weight is about 500 pounds. Earlier designs were rejected because the phase angle of the transmitted radiation did not return to its original value after the plasma cleared away. This constitutes a sensitive test for ruggedness.

The cutoff tubes must be made large enough in diameter to offer a minimum interference with the flow patterns induced by the pellet flight. Since the flow problem is part of the subject

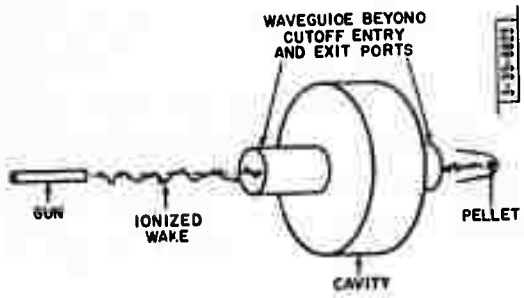

Fig. 1. Resonant cavity configuration.

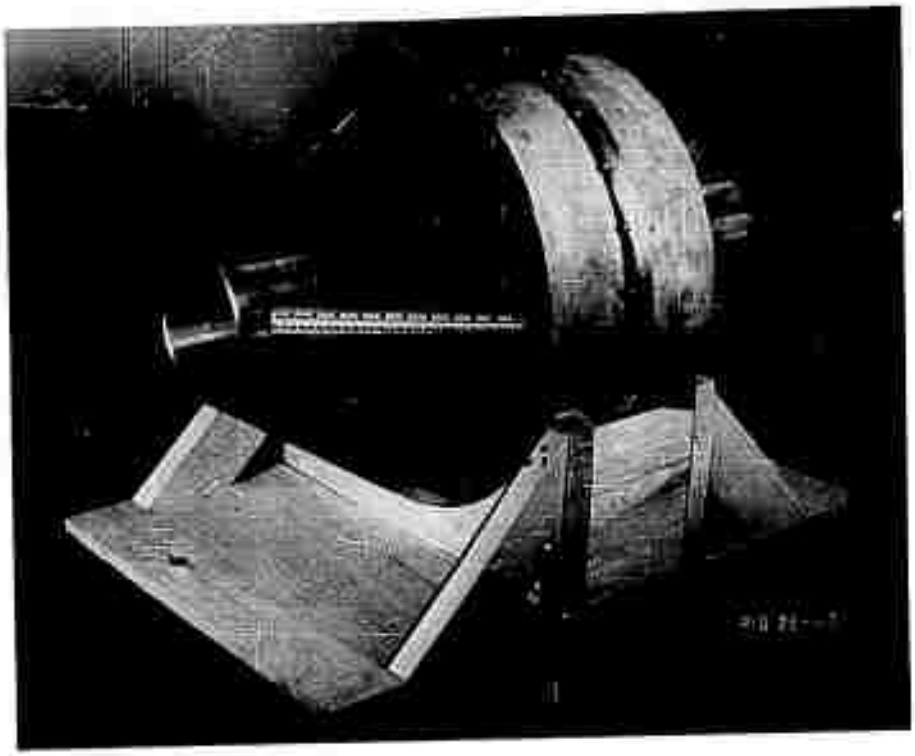

Fig. 2. Photograph of cavity.

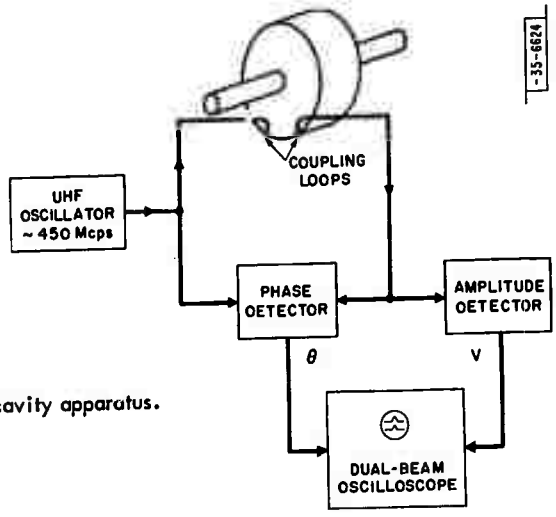

Fig. 3. Simplified black diogram af cavity apparatus.

under investigation, it is difficult to estimate the extent of this interference in advance. Feldman[3] has given results of computations of flow fields for a similar case, which show that the wake reaches sonic values at a distance of approximately 50 pellet radii behind the pellet. Beyond this region the shock is very weak and the velocity profile is stabilized. The shock is less than 10 pellet radii from the axis of flight, and the velocity profile decays to ambient in about 5 pellet radii from the axis. Our experiments have employed $\frac{1}{4}$-inch-diameter pellets, and 6-inch-diameter cutoff tubes, placing the tubes at a distance of 24 pellet radii from the axis. The interaction of the flow with the cavity should therefore be small.

III. CAVITY INSTRUMENTATION

The wake electron density and electron-molecule collision frequency are derived from a measurement of the transadmittance and a knowledge of the fixed parameters of the cavity. A simplified block diagram of the apparatus is shown in Fig. 3.

A CW signal from a 450-Mcps signal generator excites the cavity in the TM_{010} mode by means of a magnetic coupling loop. A sample of the field is coupled out with a similar coupling loop. Both the output signal amplitude and its phase relative to the input signal are presented simultaneously on a dual-beam oscilloscope. The traces are recorded photographically. In the actual system, the output of the cavity is converted to an intermediate frequency of 30 Mcps, where it is relatively simple to construct a phase detector. The detailed block diagram is shown in Fig. 4.

IV. CAVITY AND CIRCUIT ANALYSIS

The present discussion is implemented by an equivalent circuit derived from a normal mode analysis of the cavity by using the basic field equations.[2,4] Equation (5.4) of Ref. 4 (p. 78) gives the input impedance of a resonant cavity with an arbitrary number of waveguides coupled to the cavity. This equation is repeated here for two outputs. Only one mode of the cavity is considered to be strongly excited, and this is accomplished by operation near its resonant frequency with all other mode frequencies well removed. The impedances of these other modes are small series values, slowly changing with frequency, and can be lumped into the coupling coefficients, or external Q's, of the two outputs and the resonant frequency of the excited mode. Under these conditions the input admittance becomes

$$Y_g = Y_{chg} Q_g \left[\frac{1}{Q_c} + j\left(\frac{\omega}{\omega_o} - \frac{\omega_o}{\omega}\right) + \frac{1}{\epsilon_o \omega_o} \frac{\int_{v_c} J \cdot E_a \, dv}{\int_{v_c} E \cdot E_a \, dv} + \frac{1}{Q_d} \right] , \qquad (1)$$

where the subscript g refers to the waveguide into which the admittance is measured, d refers to the other coupled waveguide, Y_{chg} is the characteristic admittance of waveguide g, Q_c is the unloaded Q of the cavity in the absence of plasma, ω_o is the resonant angular frequency of the excited mode, ϵ_o is the electric permittivity of free space (mks rationalized units), J is the conduction current density of the plasma, E_a is the unperturbed electric field of the cavity, E is the field as perturbed by the plasma, v_c is the cavity volume, and Q_g and Q_d are the external Q's, or coupling Q's, of the two outputs.

An impedance model of the cavity behavior involves the definitions of voltage and current values, the ratios of which define the impedances, in terms of the electric and magnetic fields.

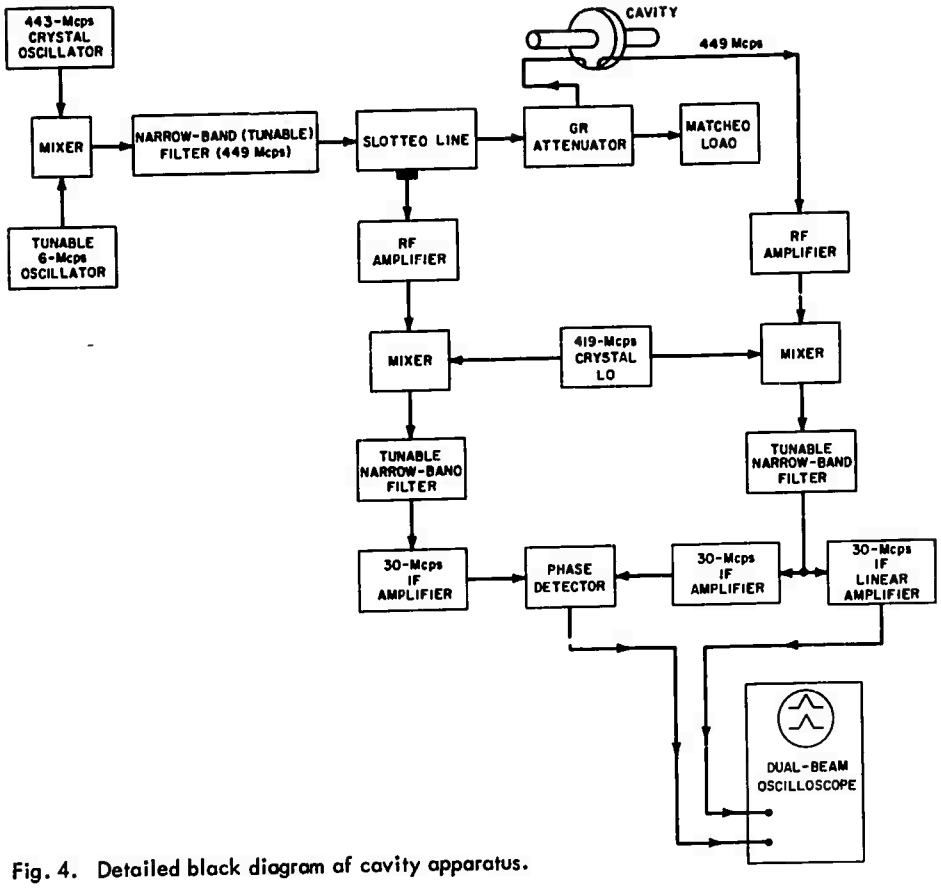

Fig. 4. Detailed black diagram of cavity apparatus.

The waveguide characteristic admittances Y_{ch} may be defined as ratios of line integrals of the fields along appropriate paths in the waveguide, or simply as products of fields measured at reference points in the guides times the characteristic dimensions. This arbitrariness never becomes a problem in the final presentation of data, since voltage ratios, current ratios and phase angles always turn out to be the desired quantities. In the present case of the TM_{010}-mode cavity, the constancy of the electric field along the axial coordinate of the cavity suggests referring all impedances and voltages to the center of the cavity, as though the points at the centers of the end plates were terminals in the circuit. The voltage difference across the cavity is then $V = E_o\delta$, where E_o is the field at the center of the cavity and δ is the length of the cavity. Voltage levels in the output lines are proportional to this value. The present definition, although arbitrary, has the merit of easy and plausible reference to the electric field of the cavity.

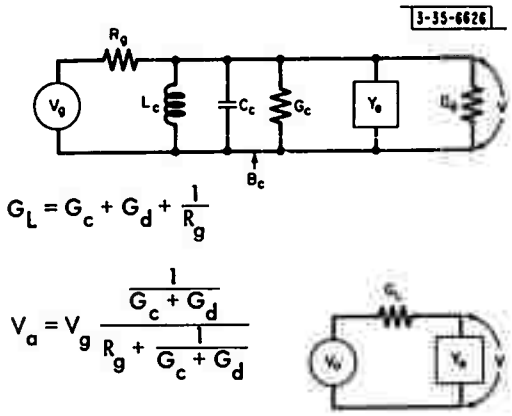

Fig. 5. Equivalent circuit of cavity (upper) and Thevenin equivalent at resonance (lower).

The various additive terms in the admittance expression of Eq. (1) imply the upper circuit of Fig. 5. The conduction currents in the plasma are accounted for by a complex admittance $Y_e = G_e + jB_e$, which is connected in parallel with the intrinsic shunt admittance $Y_c = G_c + jB_c$ of the cavity. The cavity is excited by a generator represented by the constant voltage source V_g (complex amplitude) and the series impedance R_g (real for a matched generator as used in the experiment). This generator excites the cavity through a coupling loop or other coupling device, which refers the actual values of V_g and R_g to the impedance level defined at the cavity end plates previously discussed. The intrinsic admittance of the cavity in the absence of the plasma consists of a constant real part G_c, representing the ohmic losses of the cavity, and an imaginary part

$$B_c = \omega C_c - \frac{1}{\omega L_c} = \omega_o C_c \left(\frac{\omega}{\omega_o} - \frac{\omega_o}{\omega}\right) \quad , \tag{2}$$

where L_c and C_c are the inductance and capacitance of the equivalent circuit and $\omega_o = 1/\sqrt{L_c C_c}$ is the resonant frequency. The detector admittance, again real for a matched detector, is G_d, referred to the cavity-center reference point.

The equivalent capacitance of the cavity C_c depends on the definition of the voltage which appears between its terminals. The present definition, $V = E_o\delta$, leads directly to an expression for C_c. At the instant when the magnetic field, which is in time quadrature with the electric field,

is zero, the entire cavity energy is stored in the electric field. At this instant the energy stored in the capacitance is $U = \frac{1}{2} C_c E_o^2 \delta^2$. The energy is now computed from the electric field to determine C_c. The electric field as a function of radial coordinate r for the TM_{010} mode is given by

$$E = E_z = E_o J_o\left(\frac{\alpha r}{\rho}\right) \quad ,$$

where E_o is the electric field amplitude at the center of the cavity, ρ is the radius of the cavity, J_o is the Bessel function of zero order and $\alpha = 2.405$ is the first root of $J_o(\alpha) = 0$. The electric field is independent of the axial variable. The total energy stored in the cavity is then

$$U = (1/2)\,\epsilon_o \int_o^{\rho} \left[E_o J_o\left(\frac{\alpha r}{\rho}\right)\right]^2 \delta 2\pi r \, dr$$

$$= \frac{\pi}{2}\,\epsilon_o E_o^2 \delta \rho^2 J_1^2(\alpha) \qquad (3)$$

where numerically,

$$J_1^2(\alpha) = 0.2695 \quad .$$

Equating this expression to the energy as given in terms of the circuit parameters, we obtain

$$C_c = \frac{\pi J_1^2(\alpha)\,\epsilon_o \rho^2}{\delta} \quad .$$

Using the equation for the frequency of the TM_{010} mode

$$\frac{\omega_o \rho}{c} = \alpha \quad , \qquad (4)$$

we have

$$\omega_o C_c = \pi \alpha J_1^2(\alpha)\,\frac{\rho}{\delta}\sqrt{\frac{\epsilon_o}{\mu_o}} \quad . \qquad (5)$$

The cavity susceptance becomes, finally,

$$B_c = \pi \alpha J_1^2(\alpha)\,\frac{\rho}{\delta}\sqrt{\frac{\epsilon_o}{\mu_o}}\left(\frac{\omega}{\omega_o} - \frac{\omega_o}{\omega}\right) \quad . \qquad (6)$$

Comparison with Eq. (1) shows the equivalence between $Y_{chg} Q_{eg}$ and $\omega_o C_c$, as expressed in Eq. (5). This factor also multiplies all other terms in Eq. (1). The other circuit parameters are therefore identified as:

$$G_c = \frac{\omega_o C_c}{Q_c} \quad , \qquad (7)$$

$$G_g = \frac{\omega_o C_c}{Q_g} = \frac{1}{R_g} \quad , \qquad (8)$$

$$G_d = \frac{\omega_o C_c}{Q_d} \quad , \qquad (9)$$

$$Y_e = G_e + jB_e = \frac{C_c}{\epsilon_o} \frac{\int_{V_c} J \cdot E_a \, dv}{\int_{V_c} E \cdot E_a \, dv} \quad . \tag{10}$$

The plasma admittance is computed in terms of the plasma conductivity given (in the approximation that ν_m is constant) by[2,5]

$$\sigma = \sigma_r + j\sigma_i = \frac{ne^2}{m} \frac{1}{\nu_m + j\omega} \quad , \tag{11}$$

where e is the electron charge, n is the electron density, m is the electron mass, and ν_m is the electron-molecule collision frequency for momentum transfer. Assuming that the electron density is independent of the axial coordinate z, and that the electrons are found only near the center of the cavity where $E \simeq E_o$, and noting again that $\frac{1}{2} C_c E_o^2 \delta^2 = \frac{1}{2} \epsilon_o \int_{V_c} E^2 \, dv$, we find

$$Y_e = \frac{1}{\delta} \int_o^{\rho_e} \sigma(r) \, 2\pi r \, dr = \frac{N}{\delta} \frac{e^2}{m} \frac{1}{\nu_m + j\omega} \quad , \tag{12}$$

where ρ_e is the radius of the plasma column and $N = \int_o^{\rho_e} n(r) \, 2\pi r \, dr$ is the number of electrons per unit length of plasma trail. Separating Eq. (12) into real and imaginary parts,

$$G_e = \frac{N}{\delta} \frac{e^2}{m} \frac{\nu_m}{\nu_m^2 + \omega^2} \tag{13a}$$

$$B_e = -\frac{N}{\delta} \frac{e^2}{m} \frac{\omega}{\nu_m^2 + \omega^2} \quad . \tag{13b}$$

The plasma is characterized by two parameters, N and ν_m, the determination of which is the objective of the measurement. The plasma admittance comprises a real and an imaginary part, both of which can be measured, and which are given by Eqs. (13a) and (13b). These equations can be solved simultaneously for N and ν_m, using experimental values of G_e and B_e. In the experimental situation, however, it is convenient to deal directly with the change of amplitude of the output voltage and the shift of its phase. We therefore determine first the expressions for G_e and B_e in terms of the output amplitude and phase changes, and then solve for N and ν_m.

The lower circuit of Fig. 5 gives the Thevenin equivalent of the upper circuit when the generator frequency is adjusted to the undisturbed resonant frequency of the cavity. The generator emf is $V_o = V(Y_e = 0)$, and the series admittance is $G_L = G_c + G_d + 1/R_g$, which is the total conductive load of the cavity. The series admittance may be expressed in terms of the loaded Q as

$$G_L = \frac{\omega_o C_c}{Q_L} \quad . \tag{14}$$

The ratio of the output voltage V to its value V_o when $Y_e = 0$ is

$$\frac{V}{V_o} = \frac{1/Y_e}{(1/Y_e) + (1/G_L)} = \frac{G_L}{G_L + G_e + jB_e} \quad . \tag{15}$$

The magnitude of this ratio, one of the measured quantities, is given by either of

$$S = \left|\frac{V}{V_o}\right| = -\frac{G_L}{B_e}\sin\Theta \tag{16a}$$

$$= \frac{G_L}{G_L + G_e}\cos\Theta \quad , \tag{16b}$$

where Θ is the change of phase of V from that of V_o, given by

$$\tan\Theta = -\frac{B_e}{G_L + G_e} \quad . \tag{17}$$

Using Eqs. (5) and (14),

$$S = \frac{\cos\Theta}{1 + \frac{Q_L}{\pi\alpha J_1^2(\alpha)}\frac{\delta}{\rho}\sqrt{\frac{\mu_o}{\epsilon_o}}\,G_e}$$

$$= -\frac{\pi\alpha J_1^2(\alpha)}{Q_L B_e}\frac{\rho}{\delta}\sqrt{\frac{\epsilon_o}{\mu_o}}\sin\Theta \quad .$$

Solving for G_e and B_e,

$$G_e = \frac{\pi\alpha J_1^2(\alpha)}{Q_L}\frac{\rho}{\delta}\sqrt{\frac{\epsilon_o}{\mu_o}}\left(\frac{\cos\Theta}{S} - 1\right) \tag{18a}$$

$$B_e = -\frac{\pi\alpha J_1^2(\alpha)}{Q_L}\frac{\rho}{\delta}\sqrt{\frac{\epsilon_o}{\mu_o}}\frac{\sin\Theta}{S} \quad . \tag{18b}$$

These equations provide the circuit representations of the plasma G_e and B_e in terms of the observable quantities S and Θ. These values are now equated to the equivalent quantities in Eqs. (13a) and (13b) given in terms of the plasma parameters. The resulting pair of equations are solved for the plasma parameters in terms of the measured quantities S and Θ, with the following result:

$$\nu_m = \omega\frac{\cos\Theta - S}{\sin\Theta} \tag{19}$$

$$N = \frac{\pi m}{\mu_o e^2}\frac{\alpha^2 J_1^2(\alpha)}{Q_L}\left[1 + \left(\frac{\cos\Theta - S}{\sin\Theta}\right)^2\right]\frac{\sin\Theta}{S} \quad . \tag{20}$$

Numerically, $\alpha^2 J_1^2(\alpha)\,(\pi m/\mu_o e^2) = 1.383 \times 10^{14}\,m^{-1}$ or $1.383 \times 10^{12}\,cm^{-1}$. (As a matter of curiosity, this coefficient may be compared with the reciprocal of the classical electron radius $r_o = \mu_o e^2/4\pi m$.) It is noted that the electron line density N, in electrons per unit length, is given by this technique, with no information on the radial distribution of electrons or trail diameter. If the trail diameter exceeds the diameter of the region of nearly constant electric field, the procedure yields the value of

$$\int_o^{\rho_e} E^2(r)\,n(r)\,2\pi r\,dr \quad .$$

V. LIMITATIONS AND PRECAUTIONS

A. Breakdown of Perturbation Theory

The equivalent circuit of the cavity and conducting plasma (Fig. 5) and the expression for the plasma admittance [Eq. (12)] are obtained under the small perturbation assumption that the cavity electric field is not greatly disturbed by the presence of the conducting plasma. Two criteria may be applied to determine whether this assumption is valid. First, the cavity must not be perturbed over-all to the point where its resonant frequency is changed a large fraction of its undisturbed value, or its Q is reduced to the neighborhood of unity. These two restrictions may be combined into the condition that

$$\left| \frac{1}{Q_e} + j \left(\frac{\omega}{\omega_o} - \frac{\omega_o}{\omega} \right) \right| \ll 1 \quad , \tag{21}$$

where Q_e is the contribution to the cavity Q for which the plasma is responsible, ω_o is the resonant frequency as perturbed by the electrons and ω is the original resonant frequency, equal to the applied frequency. This condition may be expressed in terms of the equivalent circuit parameters defined in Eqs. (5) and (12):

$$|Y_e| \ll \omega_o C_c \quad ,$$

which reduces to

$$N \ll \alpha^2 J_1^2(\alpha) \frac{\pi m}{\mu_o e^2} \sqrt{1 + \nu_m^2/\omega^2} \quad . \tag{22}$$

This quantity has already been seen in Eq. (20). It is concluded that the cavity is not seriously perturbed until the line density of electrons approaches the order of $10^{12}\,cm^{-1}$, or higher if ν_m exceeds ω.

In applying perturbation theory to cavities, it is necessary to consider not only the over-all perturbation of the cavity fields, but also the local perturbation. For example, a small, perfectly conducting object changes the cavity frequency only a slight amount, but causes a very large local perturbation in the vicinity of the object. A sufficient, but unduly restrictive, condition for negligible local perturbation is that the effective dielectric coefficient of the plasma be near unity. The effective dielectric coefficient of a medium of conductivity σ is given by

$$\kappa = 1 + \frac{\sigma}{j\omega\epsilon_o} \quad . \tag{23}$$

The conductivity for a plasma is given by Eq. (11). The near-unity condition on dielectric coefficient is equivalent to

$$\left| \frac{\sigma}{\omega\epsilon_o} \right| \ll 1 \quad , \tag{24}$$

or, using Eq. (11),

$$n \ll \frac{m\epsilon_o\omega^2}{e^2} \sqrt{1 + \nu_m^2/\omega^2} \quad . \tag{25}$$

In the collisionless case $\nu_m = 0$, this expression reduces to the familiar plasma frequency condition

$$\omega_p^2 = \frac{ne^2}{m\epsilon_o} \ll 1 \quad . \tag{26}$$

Condition (24) can be relaxed for the wake instrumentation configuration of cavity fields. The electric field of the cavity is parallel to the wake axis, so that the field inside the wake region is continuous with the outside field. Condition (24) restricts the conduction current density of the electrons, $J = \sigma E$, to values small compared with the Maxwellian displacement current density $J_d = j\omega\epsilon_o E$. However, even when the conduction current becomes larger than the displacement current, the radius of the plasma may be so small that the penetration of the electric field is complete and no significant attenuation or phase shift occurs over the short distance. This statement holds if the propagation factor $\exp[j\omega\sqrt{\kappa}/c]\,\rho_e$ is near unity, or

$$\left| \frac{\omega\sqrt{\kappa}}{c}\,\rho_e \right| \ll 1 \quad . \tag{27}$$

Using Eqs. (23) and (11), and taking $|\sigma| \gg \omega\epsilon_o$, this condition reduces to[6,7]

$$N = \pi\rho_e^2 n \ll \frac{\pi m}{\mu_o e^2}\sqrt{1 + \nu_m^2/\omega^2} \quad , \tag{28}$$

which is substantially the same as the large complex Q condition (22). Condition (28), along with the parallel E-field configuration, is a sufficient condition for small perturbation.

That (28) is less restrictive than (25) may be seen by finding the frequency at which they become equal:

$$\frac{\pi m}{\mu_o e^2}\sqrt{1 + \nu_m^2/\omega^2} = \pi\rho_e^2\,\frac{m\epsilon_o\omega^2}{e^2}\sqrt{1 + \nu_m^2/\omega^2} \quad ,$$

or

$$\frac{\omega\rho_e}{c} = 1 \quad , \tag{29a}$$

or

$$\lambda = \frac{2\pi c}{\omega} = 2\pi\rho_e \quad , \tag{29b}$$

where λ is the free-space wavelength. This result shows that, for plasma radii much smaller than $\lambda/2\pi$, which is the case when a plasma is contained within a low mode cavity, condition (28) is less restrictive than condition (25).

Strictly speaking, condition (25) is not correct anyway. A high mode cavity, whose dimensions are large compared with the free-space wavelength, might fulfill condition (25) but not (28). The conduction current would then be small in comparison with the displacement current, but the extent of space including the plasma would be so large that the cumulative effect of the locally small conduction current on the amplitude or phase of the propagating wave would invalidate the perturbation assumption.

A final comment on the use of perturbation theory concerns extension of the theory to a higher order of perturbation or recourse to a more exact analysis. Although a modest improvement in the range of usefulness of the technique might be achieved in this way, a basic limit lies in the loss of sensitivity of the method when the plasma is so dense that the field is either reflected or absorbed, and therefore does not penetrate at all. This limit does not lie far beyond the breakdown point of perturbation theory. A more accurate analysis of a low pressure plasma, with few collisions, and a small electron density gradient, might permit the plasma to be probed more extensively, but the cavity technique is probably not the best method for doing so.

B. End Effects

The foregoing analysis of the circuit representation of the plasma in the cavity assumed an axially homogeneous plasma aligned with the electric field. This assumption does not hold near the cavity ends, where the cutoff portals distort the field to provide a radial component of field. A simple and rough estimate of this end effect may be made by using the circuit approximation of Fig. 6. A short length of coaxial capacitance C_s is regarded to be connected in series with the

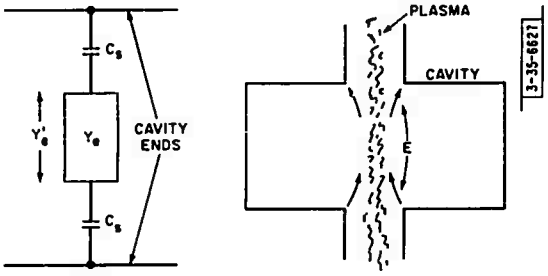

Fig. 6. Circuit with end capacitance.

electron admittance Y_e at each end. The inner and outer radii of the coaxial capacitance are the plasma radius ρ_e and the cutoff portal radius ρ_p, respectively. The length of the capacitance is more difficult to identify, but is designated by δ_s. The series value of two such capacitances, one at each end, is given by

$$\frac{C_s}{2} = \frac{\pi \epsilon_o \delta_s}{\ln(\rho_p/\rho_e)} \quad . \tag{30}$$

The admittance of these capacitances in series with the plasma admittance Y_e is given by

$$\frac{1}{Y'_e} = \frac{1}{j\omega(C_s/2)} + \frac{1}{Y_e}$$

or

$$Y'_e = \frac{Y_e}{1 + (2Y_e/j\omega C_s)} \quad . \tag{31}$$

It is noted that, when collisions are absent, Y_e is a negative imaginary number and Eq. (31) has a resonant denominator. Collisions modify the resonance in a conventional way.

The condition for small end effects is that the second term in the denominator of (31) be small in magnitude compared with unity. This condition is equivalent to saying that the series impedance of the capacitances be small compared with the plasma impedance. Using Eq. (30) to compute the former and Eq. (12) to compute the latter, the condition becomes

$$N \ll \frac{\pi m}{\mu_o e^2} \sqrt{1 + \nu_m^2/\omega^2}\, \frac{\omega^2 \delta \delta_s}{c^2 \ln(\rho_p/\rho_e)} \quad . \tag{32}$$

This expression differs from (28) by the factor $\omega^2 \delta \delta_s / c^2 \ln(\rho_p/\rho_e)$. The logarithm is not much greater than unity, even for fairly large radius ratios. If δ and δ_s are of the order of $\lambda/2\pi$, the entire factor is also of the order of unity. Cavity dimensions are usually taken of this order. The new condition is therefore substantially the same as the previous conditions (22) and (28). If the cavity is made short (pancake shaped) the series-capacitance limitation is more stringent.

The series-capacitance effect may be estimated in a different manner, which affords a different point of view as well as another approach to selecting the dimensions to put into the expression (32). This method considers the part of the plasma which is exposed to the electric field of the cavity as a prolate spheroid with major semiaxis $\delta/2$ and minor semiaxis ρ_e. If condition (28) holds, the region containing the plasma may be treated quasistatically; that is, the electrostatic depolarizing effect of the body shape may be used to compute the field inside the plasma in terms of the field outside (identified with the "field at infinity" in the corresponding electrostatic problem). The spheroid is therefore characterized by a depolarizing factor ℓ given by[8]

$$\ell = \frac{1-\mathcal{E}^2}{2\mathcal{E}^3} \left(-2\mathcal{E} + \ln \frac{1+\mathcal{E}}{1-\mathcal{E}}\right) \quad , \tag{33}$$

where $\mathcal{E}$ is the eccentricity given by

$$\mathcal{E} = \sqrt{1 - 4\rho_e^2/\delta^2} \quad . \tag{34}$$

The field E_i inside the plasma is given in terms of the external field E_o and the equivalent polarization

$$P = \epsilon_o \frac{\sigma}{j\omega\epsilon_o} E_i$$

as

$$E_i = E_o - \ell \frac{P}{\epsilon_o} = E_o - \ell \frac{\sigma}{j\omega\epsilon_o} E_i \quad .$$

Solving for E_i,

$$E_i = \frac{E_o}{1 + \ell(\sigma/j\omega\epsilon_o)} \quad . \tag{35}$$

We now return to Eq. (10), and use the modified internal field of Eq. (35) to compute the current density J. The denominator is treated as before, since the integral here contains contributions to the integrand from all regions of the cavity, in contrast with the situation in the integral of the numerator where the integrand is zero except where the conducting material is present to alter the field. As before, $C_o/\epsilon_o \int_{v_c} E^2 dv = 1/E_o^2 \delta^2$, but now $J = \sigma E_i$. Thus

$$Y_e' = \frac{Y_e}{1 + (\ell \delta Y_e / j\pi\omega\epsilon_o \rho_e^2)} \quad , \tag{36}$$

where $Y_e = \pi\rho_e^2\sigma/\delta$. In this expression the integration is simplified by the assumption that the conductivity is constant throughout the plasma to the radius ρ_e. The shape is assumed cylindrical in the integration, even though it was taken to be spheroidal to obtain ℓ. It is noted that, in the collisionless case, Eq. (36) has a resonant denominator, as was true of Eq. (31).

Equation (36) is now compared with Eq. (31) to obtain the equivalent value of C_s:

$$C_s = \frac{2\pi\epsilon_o\rho_e^2}{\ell\delta} \quad .$$

Substituting the value of ℓ from the leading term in the expansion of Eq. (33) in the small quantity ρ_e/δ

$$\ell = \frac{4\rho_e^2}{\delta^2} \ln\frac{\delta}{\epsilon\rho_e} \quad ,$$

we obtain

$$C_s = \frac{\pi\epsilon_o\delta}{2\ln(\delta/\epsilon\rho_e)} \quad , \tag{37}$$

where $\epsilon = 2.718\ldots$ is the Naperian logarithm base.

Equation (37) may be compared with Eq. (30). The length δ_s of the coaxial condenser appears here as one-fourth of the cavity length, and there is a minor difference in the logarithmic term. The coaxial condenser envisions different field details from those of the spheroid, and neither is an exact description of the real fields. However, the conclusion in the paragraph following Eq. (32) is supported by either approach, so that the concept of a series-capacitance effect and the order of magnitude of the upper limit of electron density imposed by the effect are reasonably well established.

C. Surface-Wave Coupling Through Portals

The portal tubes through which the pellet passes are chosen of sufficiently small diameter to be well into the cutoff region, to prevent electromagnetic energy from escaping through this route from the cavity. However, when the effective dielectric coefficient of the plasma is sufficiently low, a surface-wave, or slow-wave, type of propagation can take place.[9] In a lossless plasma this wave propagates at $\kappa \leqslant -1$, being strictly confined to the surface when $\kappa \approx -1$. With reduction of κ below -1, the fields penetrate further into the regions away from the surface. Outside the plasma this trend continues indefinitely, but inside the penetration reaches a maximum and then decreases. As κ approaches $-\infty$, the fields inside the plasma become surface fields again, whereas the outside fields become identical with those of a coaxial line made of perfect conductors. The physical basis of these surface waves lies in the characteristic which a medium of negative dielectric coefficient has of accumulating positive charges at the tails of the E-lines rather than at the heads. These E-lines can thus leave positive surface charges, which they produce, on both sides of the plasma-free-space interface, and terminate on similarly produced negative charges. The surface charge wave is peristaltic.

Since such a propagating mode can exist, the effectiveness of the "cutoff" tubes is questionable. In order to estimate the seriousness of this effect, we compare twice the characteristic impedance of such a wave with the impedance of the plasma. If the former is small in comparison

with the latter, the impedance of the series coaxial lines cannot falsify the measured values of plasma impedance. The actual impedance reflected from the coaxial line into the cavity depends on the impedance that the line sees on the outside, and is equal to the characteristic impedance only if the line is matched. However, the order of magnitude of electron density at which this effect is important can at least be estimated by this comparison. Although the analysis is not carried through here, the results are presented.

Near the onset of propagation, where κ is equal to or slightly less than -1, the fields are closely confined to the region near the surface. The electric and magnetic fields are disposed in the same directions as in the usual coaxial TEM mode. The current in the line is obtained by a line integral of the magnetic field around the plasma inner conductor at the interface. Since this integral is taken at the surface where the magnetic field is nonvanishing, it is of normal size. The potential difference, on the other hand, is a line integral of the electric field along a radial path from the interface to the outer conductor. Since the field drops rapidly in going away from the surface, the potential difference is very small. The characteristic impedance, which is the ratio of potential difference to current, is therefore also small.

As the electron density is increased beyond this value, and κ drops further below -1, the characteristic impedance rises owing to the increasing penetration of the electric field toward the outer conductor. It can be shown that, in the intermediate region, where $\kappa \ll -1$ but $N \ll \pi m/\mu_o e^2$, the characteristic impedance is given approximately by

$$Z_{ch} = \sqrt{\frac{\mu_o}{\epsilon_o}} \sqrt{\frac{m}{2\pi\mu_o e^2 N} \ln \frac{\rho_p}{\rho_e}} \quad . \tag{38}$$

Since this value decreases with increasing N, Z_{ch} must pass through a maximum. As N goes beyond the value $\pi m/\mu_o e^2$ toward infinity, Eq. (38) no longer holds, but rather Z_{ch} levels out to the value for the simple coaxial line

$$Z_{ch} = \frac{1}{2\pi} \sqrt{\frac{\mu_o}{\epsilon_o}} \ln \frac{\rho_p}{\rho_e} \quad . \tag{39}$$

The plasma impedance for the lossless case ($\nu_m = 0$) is given by

$$Z_e = \frac{\delta}{\pi \rho_e^2 \sigma} = j \frac{\omega m \delta}{\pi \rho_e^2 n e^2} = j \frac{\omega m \delta}{N e^2} \quad . \tag{40}$$

If we require the magnitude of Z_e to be large compared with twice the characteristic impedance as given by Eq. (38), we obtain

$$N \ll \frac{\pi m}{\mu_o e^2} \frac{\omega^2 \delta^2}{c^2} \frac{1}{2 \ln(\rho_p/\rho_e)} \quad . \tag{41}$$

Since δ is of the order of $\lambda/2\pi$, and the ln-factor cannot be greatly different from unity, the slow-wave effect begins to be a problem when N approaches $10^{12}\,cm^{-1}$. However, this is just where Z_{ch}, as given by Eqs. (38) and (39), agrees owing to the leveling off, so that we could just as well have required that (40) be large compared with twice (39), resulting in

$$N \ll \frac{\pi m}{\mu_o e^2} \frac{\omega \delta}{c} \frac{1}{\ln(\rho_p/\rho_e)} \quad . \tag{42}$$

If electron line densities well below 10^{12} cm^{-1} are measured, little difficulty may be expected from the portal impedances. However, another possible effect of the slow-wave propagation may occur within the cavity itself. The wave velocity is zero at $\kappa = -1$, and rises as κ decreases until, at $-\infty$, it reaches the free-space propagation velocity c. It is this behavior which leads to the term "slow wave." One can therefore visualize an entire series of new cavity modes using the slow-wave propagation mechanism. If one of these modes coincides in frequency with the applied frequency (that of the undisturbed TM_{010} mode), it will also be excited. The degree of excitation will depend on the relative field configurations of the two modes. It seems reasonable that the coupling will be related to the common impedances, so that the criterion (42) for weak external coupling through the portal tube must be similar to the criterion for excitation of slow-wave resonances. If this surmise is correct, similar electron densities are required.

D. Electron Heating by the RF Field and Measurement Sensitivity

If the components of the measurement system are well engineered for stability and isolation from external disturbance, the ultimate sensitivity of the measurement of electron density and collision frequency is determined by the comparison between the front-end noise of the amplitude and phase detectors and the output signal of the cavity. The cavity output signal can always be increased by an increase in the signal generator power. The limitation becomes the maximum power that can be absorbed by the cavity without exceeding the permissible disturbance to the electron energy distribution function. Heating of the electrons by the cavity fields is therefore of interest in determining the sensitivity and accuracy of the experiment.

The power per unit volume delivered to the electrons by the cavity field is given by

$$P = \frac{1}{2}\sigma_r E_o^2 = \frac{ne^2\nu_m E_o^2}{2m(\nu_m^2 + \omega^2)} \quad ,$$

where σ_r is the real part of the complex conductivity of the plasma, given by Eq. (11). This value is proportional to the electron density and to the collision frequency; therefore, the energy delivered to each electron at each collision is

$$\Delta u_E = \frac{e^2 E_o^2}{2m(\nu_m^2 + \omega^2)} \quad .$$

The energy transfer from the field to the electron is associated with the collision process because the in-phase component of the velocity of the electron is generated only in the collisional deflection. In the absence of collisions, the velocity is in time-quadrature to the electric field.

The energy lost in an elastic collision between an electron of mass m and a molecule of mass M due to elastic recoil, on the average, is given by .

$$\Delta u_c = -\frac{2m}{M}\Delta u \quad ,$$

where Δu is the amount by which the electron kinetic energy exceeds that of the molecule. Diatomic molecules are excited into rotational and vibrational states even at low energies, so that the mass ratio 2m/M is replaced by a larger factor g which is best determined experimentally. Huxley and Zaazou report $g = 1.3 \times 10^{-3}$ for air in the energy range of 0.2 to 0.8 ev (see Ref. 10). The steady-state increment of electron energy above the ambient thermal energy is given by

$$\Delta u_E + \Delta u_c = 0$$

or

$$\Delta u = \frac{e^2 E_o^2}{2mg(\nu_m^2 + \omega^2)} \quad .$$

The maximum field E_o which may be applied if Δu is the maximum permissible increment of electron energy is therefore

$$E_o = \sqrt{\frac{2mg\Delta u(\nu_m^2 + \omega^2)}{e^2}} \quad . \tag{43}$$

This result may be expressed in terms of the maximum incident power from the signal generator

$$P_i = \frac{V_g^2}{8R_g} = \frac{V^2}{8} \frac{Q_g}{Q_L^2} \omega_o C_c \quad .$$

This expression holds only when electrons are sparse or absent. Using $V = E_o\delta$, solving for E_o, equating to (43), and finally solving for P_i,

$$P_i = \frac{1}{4} \alpha^3 J_1^2(\alpha)\, g \frac{\delta}{\rho} \frac{Q_g}{Q_L^2} \left(1 + \frac{\nu_m^2}{\omega^2}\right) \frac{\pi m}{\mu_o e^2}\, c\Delta u \quad . \tag{44}$$

Typical numerical values are: $g = 1.3 \times 10^{-3}$, $\delta/\rho = 1$, $Q_g = 5000$, $Q_L = 2500$, $\nu_m/\omega = 1$, $\Delta u = 0.1 \times (3/2)\, kT$, $k = 1.38 \times 10^{-23}$ joule/degree, $T = 300°K$. The maximum incident power for these values is $P_i = 3.2 \times 10^{-5}$ watt, or 32 μwatts. More power may be applied when the electron density is high, but variation of signal generator power for optimum conditions at each electron density is very inconvenient. However, the power level computed above is always safe.

We next consider the minimum electron density which can be detected subject to the maximum excitation field as computed above. Minimum electron density implies a nearly plasma-free cavity (Y_e small). The limit is regarded as set by detector noise with a noise temperature T_d. In practice, the detector calibration is reliable only if the impedance connected to the detector input is constant, requiring a device such as a ferrite isolator between the cavity output and the receiver. With an isolator, the cavity presents a matched input impedance to the detector of $R_d = 1/G_d$ irrespective of the plasma density in the cavity or of the coupling conditions. For Y_e small, an rms noise voltage

$$V_n = \sqrt{\frac{4kT_d}{G_d \tau}} \tag{45}$$

is therefore indicated by the detector, where τ is its response time. The signal voltage is given by Eq. (15), which for $|Y_e| \ll G_L$, or, using Eqs. (12), (4), (5) and (14),

$$N \ll \frac{1}{Q_L} \alpha^2 J_1^2(\alpha) \frac{\pi m}{\mu_o e^2} \sqrt{1 + \frac{\nu_m^2}{\omega^2}} \tag{46}$$

$$V \approx V_o \left(1 - \frac{Y_e}{G_L}\right) \quad . \tag{47}$$

The magnitude of the difference voltage $V_o|Y_e|/G_L$ is compared with the noise voltage for minimum detectable electron density. Using Eq. (12) for Y_e,

$$\frac{V_o}{G_L} \frac{N}{\delta} \frac{e^2}{m} \frac{1}{\sqrt{\nu_m^2 + \omega^2}} = \sqrt{\frac{4kT_d}{G_d \tau}}$$

determines the minimum detectable N. Substituting Eq. (43) for $V_o/\delta = E_o$, using Eqs. (9), (14) and (5), and solving for N,

$$N_{min} = \sqrt{2\alpha J_1^2(\alpha) \frac{Q_d}{Q_L^2} \frac{\rho}{\delta} \frac{kT_d}{g\Delta u} \frac{\pi m}{\mu_o e^2} \frac{1}{c\tau}} \quad . \tag{48}$$

Since $V_o - V$ is proportional to N, this expression also represents the error in the measurement of N at any N consistent with (46). A typical set of numerical values is: $Q_d/Q_L^2 = 10^{-4}$, $\rho/\delta = 1$, $T_d = 900°K$, $\Delta u/k = 30°K$, $g = 1.3 \times 10^{-3}$, $\tau = 10^{-5}$ sec, giving $N_{min} = 3 \times 10^3 \text{ cm}^{-1}$.

At the opposite limiting case of $|Y_e| \gg G_L$, or

$$N \gg \frac{1}{Q_L} \alpha^2 J_1^2(\alpha) \frac{\pi m}{\mu_o e^2} \sqrt{1 + \frac{\nu_m^2}{\omega^2}} \quad , \tag{49}$$

the plasma becomes a heavy load on the cavity and the output voltage drops to a low value

$$V \approx V_o G_L / Y_e \quad . \tag{50}$$

It is of interest to see at what electron density the output voltage drops into the noise. This condition does not define a real upper limit to measurable electron density, since the signal generator power may be increased to compensate for the drop in electric field in the plasma without incurring an increase of electron energy beyond the set value of Δu. Specifically, the generator may be turned up until the new value of V is equal to the old limitation on V_o defined by Eq. (43). The ratio of permitted voltage increase, by Eq. (50), is

$$\frac{|Y_e|}{G_L} = \frac{Q_L}{\alpha^2 J_1^2(\alpha)} \frac{N}{\pi m/\mu_o e^2} \frac{1}{\sqrt{1 + \nu_m^2/\omega^2}}$$

which is of the order of Q_L for $N \approx \pi m/\mu_o e^2$, the order of the maximum N that can be measured without invalidating the perturbation assumptions. For Q_L of the order of 2500, the 32-μw incident power previously computed may be increased to 200 watts. However, it is inconvenient to design the components of the system to change characteristics with changes in electron density. It is therefore of interest to determine the maximum electron density which may be measured at a signal generator setting which does not unduly disturb the electron energy even when the electron density is low. This limit is determined by equating the magnitude of V in Eq. (50) to the noise voltage in Eq. (45). Expressing the G's in terms of the Q's and manipulating as in the computation of the low N limit,

$$N_{max} = \frac{a^{7/2} J_1^3(\alpha)}{Q_L \sqrt{Q_d}} \sqrt{\frac{\mu\omega}{2\sigma}\frac{\delta}{\rho}} \left(\frac{m}{\mu_0 e^2}\right)^{3/2} \sqrt{c\tau} \left(1 + \frac{\nu_m^2}{\omega^2}\right) \quad . \tag{51}$$

Typical numerical values of $Q_L\sqrt{Q_d} = 10^6$, and others as given above, lead to $N_{max} = 6 \times 10^{12}\ cm^{-1}$. Inasmuch as this value is beyond the small perturbation limit, it does not appear necessary to increase the signal generator power beyond the safe value in the absence of electrons.

ACKNOWLEDGMENTS

The problem of flow-field interaction with the cavity walls has been discussed with us by Dr. E. L. Murphy. The slow-wave-mode coupling mechanism from the cavity through the entry and exit portals was brought to our attention by Dr. S. Edelberg. Dr. J. Hermann has criticized extensive parts of the manuscript, made many valuable suggestions which have been incorporated into the report and bolstered our confidence by following up the analysis of some conclusions with higher approximations. Mr. H. G. Pascalar has been working on similar techniques, and we have enjoyed comparing notes with him. Our thanks are extended to these people, without implying their responsibility for possible errors.

REFERENCES

1. S. C. Brown, et al., Technical Report No. 66, Research Laboratory of Electronics, M. I. T. (17 May 1948).
2. V. E. Golant, Soviet Physics, Technical Physics 5, 1197 (1961). (Translation from Zhur. Tekn. Fiz. 30, 1265 (1960).)
3. S. Feldmon, Research Report 71, Avco-Everett Research Laboratory (June 1959).
4. J. C. Slater, Microwave Electronics, Chap. IV (Van Nostrand, New York, 1950).
5. E. V. Appleton and F. W. Chapman, Proc. Phys. Soc. (London) 44, 246 (1932).
6. S. J. Buchsbaum, L. Mower and S. C. Brown, Phys. Fluids 3, 806 (1960).
7. N. Herlofson, Rep. Prog. Phys. 11, 444 (1948); Arkiv Fysik 3, 247 (1951).
8. J. A. Stratton, Electromagnetic Theory (McGraw-Hill, New York, 1941), pp. 211-214. Note that Eq. (45) of this reference is misprinted, and should read instead $A_1 = -\frac{1}{a^3\mathcal{E}^3}\left(2\mathcal{E} - \ln\frac{1+\mathcal{E}}{1-\mathcal{E}}\right)$.
9. A. W. Trivelpiece, Technical Report No. 7, Electron Tube and Microwave Laboratory, California Institute of Technology (May 1958).
10. H. S. W. Massey and E. H. S. Burhop, Electronic and Ionic Impact Phenomena (Oxford University Press, London, 1952), p. 279.